Dongfeng L, Carstens J, Schauer T, Raisch J. **Haptic control of a table-placed mobile robot for arm/shoulder rehabilitation.** In Proc. of the 3rd European Conference Technically Assisted Rehabilitation - TAR 2011, Berlin, Germany, 2011.

Haptic control of a table-placed mobile robot for arm/shoulder rehabilitation

Dongfeng Luo[1,2,3]**, Jan Hendrik Hermann Carstens**[1]**, Thomas Schauer**[1]**, Jörg Raisch**[1,2]
[1]Technische Universität Berlin, Control Systems Group, Berlin, Germany
[2]Max Planck Institute for Dynamics of Complex Technical Systems,
Systems and Control Theory Group, Magdeburg, Germany
[3]Xi'an Institute of Optics and Precision Mechanics of CAS, Xi'an, China

Abstract – This contribution is concerned with the development and control of a portable and active rehabilitation robot for stroke patients. The table-placed mobile robot is able to guide and assist the patient's lower arm to move in a horizontal plane for elbow and shoulder training. The device offers haptic control for compliance and for implementation of a virtual therapist. Haptic control was realised in form of an admittance control scheme which utilises the measured interaction force between the patient and the robot as input to a given virtual environment. A high bandwidth position controller keeps the robot close to the position and orientation dynamically defined by the virtual environment. Sensor fusion based on an extended Kalman filter is used to estimate the absolute position of the robot on the table as well as its orientation. The feasibility of the control concept was demonstrated in experiments with neurologically intact subjects.

1 Introduction

A variety of upper limb rehabilitation robots in many forms have been developed to assist, enhance, evaluate, and document neurological and orthopaedic rehabilitation of movement, including *MIT-Manus* [1] and *ARMin* [2]. These devices have been proven to reduce motor impairment in the hemiparetic upper limbs of stroke patients. However, their development for an exclusively clinical use entails a lack of mobility, high acquisition costs and limited patient training times. To address some of these issues, new concepts that allow stroke patients with upper limbs impairments to continue rehabilitation therapy at home have been suggested in [3, 4]. Both concepts involve passive/semi-active table-top devices that are lightweight and easy to set up. However, there potential is limited by the lack of active patient support.

This paper presents the haptic control design for a novel robot-aided rehabilitation system for upper limbs called *Reha-Maus*. The *Reha-Maus* poses the first concept of a portable rehabilitation robot that actively provides different levels of patient assistance. Its compact design and reduced complexity facilitate user friendly home training as well as clinical use, and the implemented haptic control strategy offers a virtual therapist to guide and assist patient's arm training. Furthermore, its estimated low price allows for group therapy with several robots in use. Moreover, the utilised sensors and the use of computer control allow for advanced training programs and continuous patient's assessment and progress monitoring.

2 Robotic Set-up

Figure 1 shows a prospective application scenario of the *Reha-Maus*. The lower right arm of a patient is pivoted on the moving robotic platform. Human-device interaction forces are measured by a force sensor underneath the arm support. Arbitrary motion, i.e. planar robot translation and rotation, on the application surface is facilitated by three assembled omni-wheels. Their design allows for low-friction rolling perpendicular to the attached motor shaft. Each omni-wheel is driven by a DC motor (20 W) with gear and encoder. In current prototype version, separate external power electronics provide analogue current controllers for each motor. A compact, yet powerful device design is achieved by mounting the high-performance drives along the edges of an equilateral triangle. The configuration is capable of producing a predetermined range of force (0–51 N) and velocity (translational 0–0.6 m/s, rotational 0–9 rad/s). The robot weighs 2.8 kg and has a diameter of 300 mm. At this stage of development, absolute position information is gathered by an infrared camera, and the force signals are collected by a 3 DOF force sensor with a range of force (0–100 N) and torque (0–6.3 Nm). A real time Linux-based computer interface allows for the use of advanced control algorithms that have been implemented using Scilab/Scicos and the HART toolbox[1].

3 Dynamics and Kinematics

The *Reha-Maus* is a 3 DOF mobile system and has a fixed body frame $[x_r, y_r]$, aligned on the centre of mass (cf. Figure 2). The description of the dynamics take place in the generalised coordinates $\boldsymbol{q} = [x, y, \theta]'$ where x and y is the position of the robot on the workspace and θ is the orientation. To determine the equations of motion and to design position and force controllers the kinematics of the robot have to be

---

[1] http://hart.sf.net/

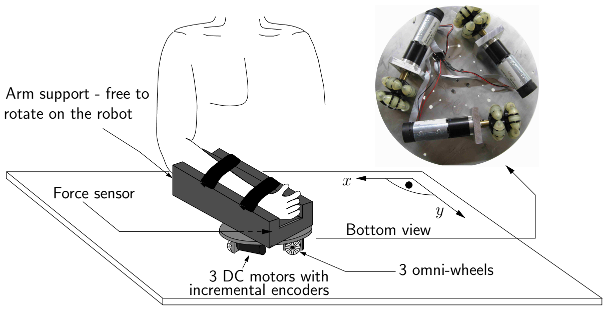

Figure 1: *Reha-Maus.*

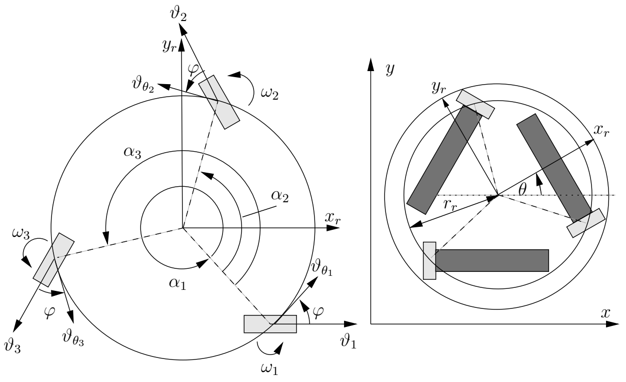

Figure 2: Geometry of the robot platform.

investigated at first. To calculate the generalised velocities $\dot{\boldsymbol{q}}$ from the vector $\boldsymbol{\omega} = [\omega_1, \omega_2, \omega_3]'$ of wheel speeds a transformation matrix $\boldsymbol{\Gamma}$ is derived. Using geometric relations (see Figure 2) translational ($\dot{x}_r(t)$, $\dot{y}_r(t)$) and the rotational ($\dot{\theta}(t)$) velocities of robot are obtained by

$$\dot{x}_r(t) = \sum_{i=1}^{3} \underbrace{r_w \cdot \omega_i(t)}_{\vartheta_i} \cdot \cos(\alpha_i), \quad \dot{y}_r(t) = \sum_{i=1}^{3} \underbrace{r_w \cdot \omega_i(t)}_{\vartheta_i} \cdot \sin(\alpha_i), \quad \dot{\theta}(t) = \frac{1}{r_r} \cdot \sum_{i=1}^{3} \underbrace{r_w \cdot \omega_i(t)}_{v_{\theta_i}} \cdot \sin(\varphi)$$

where r_w and r_r are the wheel and robot rotation radius, $\varphi = 39°$ is a construction specific angle and $\alpha_1 = 0, \alpha_2 = 2/3\pi, \alpha_3 = 4/3\pi$. This result can be also written in vector/matrix form:

$$\begin{pmatrix} \dot{x}_r \\ \dot{y}_r \\ \dot{\theta} \end{pmatrix} = r_w \underbrace{\begin{pmatrix} \cos(\alpha_1) & \cos(\alpha_2) & \cos(\alpha_3) \\ \sin(\alpha_1) & \sin(\alpha_2) & \sin(\alpha_3) \\ \frac{\sin(\varphi)}{r_r} & \frac{\sin(\varphi)}{r_r} & \frac{\sin(\varphi)}{r_r} \end{pmatrix}}_{\boldsymbol{\Gamma}_r} \begin{pmatrix} \omega_1 \\ \omega_2 \\ \omega_3 \end{pmatrix}$$

By using the transformation matrix $\boldsymbol{\Gamma}_q$ between robot coordinates and generalised coordinates, the generalised velocities $\dot{\boldsymbol{q}}$ can be computed as follows:

$$\dot{\boldsymbol{q}}(t) = r_w \underbrace{\boldsymbol{\Gamma}_q \boldsymbol{\Gamma}_r}_{\boldsymbol{\Gamma}} \boldsymbol{\omega}(t), \quad \boldsymbol{\Gamma}_q = \begin{pmatrix} \cos(\theta) & -\sin(\theta) & 0 \\ \sin(\theta) & \cos(\theta) & 0 \\ 0 & 0 & 1 \end{pmatrix}, \quad \boldsymbol{\Gamma} = \begin{pmatrix} \cos(\theta) & \cos(\theta + \frac{2\pi}{3}) & \cos(\theta + \frac{4\pi}{3}) \\ \sin(\theta) & \sin(\theta + \frac{2\pi}{3}) & \sin(\theta + \frac{4\pi}{3}) \\ \frac{\sin(\varphi)}{r_r} & \frac{\sin(\varphi)}{r_r} & \frac{\sin(\varphi)}{r_r} \end{pmatrix}$$

The inverse of $\boldsymbol{\Gamma}$ is given by

$$\boldsymbol{\Gamma}^{-1} = \begin{pmatrix} \frac{2\cos(\theta)}{3} & \frac{2\sin(\theta)}{3} & \frac{r_r}{3\sin(\varphi)} \\ -\frac{\sqrt{3}\sin(\theta)+\cos(\theta)}{3} & -\frac{\sin(\theta)-\sqrt{3}\cos(\theta)}{3} & \frac{r_r}{3\sin(\varphi)} \\ \frac{\sqrt{3}\sin(\theta)-\cos(\theta)}{3} & -\frac{\sin(\theta)+\sqrt{3}\cos(\theta)}{3} & \frac{r_r}{3\sin(\varphi)} \end{pmatrix}$$

and plays a crucial role in position and force control of the robot. It is also required if the system dynamics in generalised coordinates are determined from Euler-Lagrange equations.

4 Position control

Basis for the development of the haptic controller in Section 5 is the availability of a position controller. The position control of the *Reha-Maus* was investigated in [5] and will only be summarised in the sequel. Figure 3

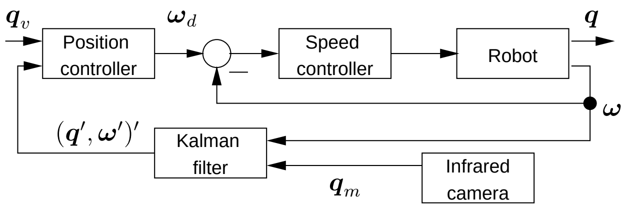

Figure 3: Position control scheme.

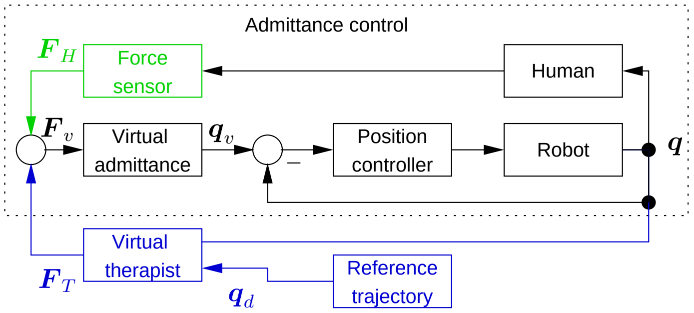

Figure 4: Admittance control scheme.

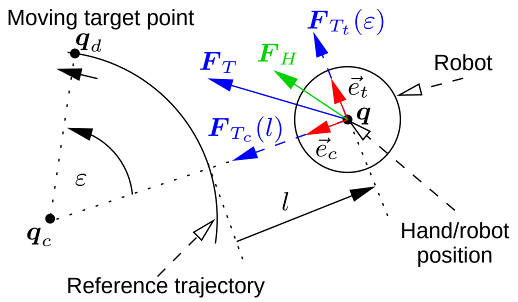

Figure 5: Force components at the hand/robot.

gives an overview about the cascaded control structure. The robot position $\boldsymbol{q}$ is estimated by sensor fusion using an extended Kalman filter those inputs are the wheel velocities (determined from motor encoders) and a time-delayed, low frequency sampled, position measurement $\boldsymbol{q}_m$ determined from an infrared camera mounted above the table. The inner loop of the cascaded control structure consists of individual speed controllers with anti-windup-schemes. For the outer loop, an optimal position controller is used based on a discrete-time Linear Quadratic Regulator (LQR) design. This controller generates reference signals for the wheel velocities in order to track a reference position $\boldsymbol{q}_r$.

5 Haptic control

Robotic arm/shoulder therapy may consist of repetitive point-to-point or cyclic movements. Latter can for example be a circle which the patient has to track. Haptic control of the robot is required for several reasons. First, physical properties of the robot like inertia and damping must be virtually modulated according to the patients skills. Second, the motion of the patient has to be restrained to a vicinity of the specified movement paths. Of course, this can be achieved by making the virtual physical parameters of the robot dependent on position. Third, if required, assistence must be provided in order to guide to patient's hand along given trajectories. This concept is called "virtual therapeut". In this paper, haptic control was realized in form of an admittance control using a force measurement at the robot and the position controller outlined before.

Using admittance control, the real dynamics of the robot shall rendered into a desired virtual dynamics (system of mass-spring-dampers) given by

$$\boldsymbol{F}_v(t) = \boldsymbol{F}_H(t) + \boldsymbol{F}_T(t) = \boldsymbol{M}_v \ddot{\boldsymbol{q}}_v(t) + \boldsymbol{D}_v \dot{\boldsymbol{q}}_v(t) + \boldsymbol{K}_v \boldsymbol{q}_v(t) \tag{1}$$

where $\boldsymbol{M}_v$, $\boldsymbol{D}_v$ and $\boldsymbol{K}_v$ are the virtual inertia, damping and stiffness matrices respectively. The desired orientation of the robot shall be kept at zero. This is achieved by setting the related entries in the matrices $\boldsymbol{M}_v$, $\boldsymbol{D}_v$ and $\boldsymbol{K}_v$ to infinity. Input to this virtual admittance model is the force vector $\boldsymbol{F}_v$ which is the superposition of the sensed interaction force vector $\boldsymbol{F}_H$ between the robot and the patient and the force vector $\boldsymbol{F}_T$ generated by the "virtual therapist". All force vectors contain three generalised force components (forces in x and y direction and torque). The desired virtual position $\boldsymbol{q}_v$ of the robot is the output of the admittance model and can be obtained by numerically integrating Eq. (1) in real time. Finally, the previously outlined position control is used to track the virtual position $\boldsymbol{q}_v$ as illustrated in Figure 4.

The virtual therapist was designed to support the movement of the patient, if required, along a given circle trajectory and to keep deviations from the desired trajectory small. To achieve these goals the shortest distance $l(t)$ between the hand position and the circle is determined together with the angle $\varepsilon(t)$ (cf. Figure 5). Latter gives a measure for the phase delay between the desired position of the hand and the actual one. The force vector $\boldsymbol{F}_T(t)$ of the virtual therapist is composed of two components. The first component $\boldsymbol{F}_{T_c}(t)$ pushes the hand/robot back to the circle in direction of the unit vector $\vec{e}_c(t)$ as shown in Figure 5. This vector always points in direction of the circle centre. The second force component $\boldsymbol{F}_{T_t}(t)$ pushes the hand/robot tangentially to the circle in direction of the unit vector $\vec{e}_t(t)$. Spring characteristics are assumed to calculate the absolute values of the two forces dependent on the distances $l(t)$ and the angle $\varepsilon(t)$ respectively. Finally, the force $\boldsymbol{F}_T(t)$ is given by

$$\boldsymbol{F}_T(t) \quad = \quad \underbrace{-k_l \, l(t) \cdot \vec{e}_c(t)}_{\boldsymbol{F}_{T_c}} + \underbrace{k_t \, \varepsilon(t) \cdot \vec{e}_t(t)}_{\boldsymbol{F}_{T_t}} \tag{2}$$

where k_l and k_ε are the spring constants.

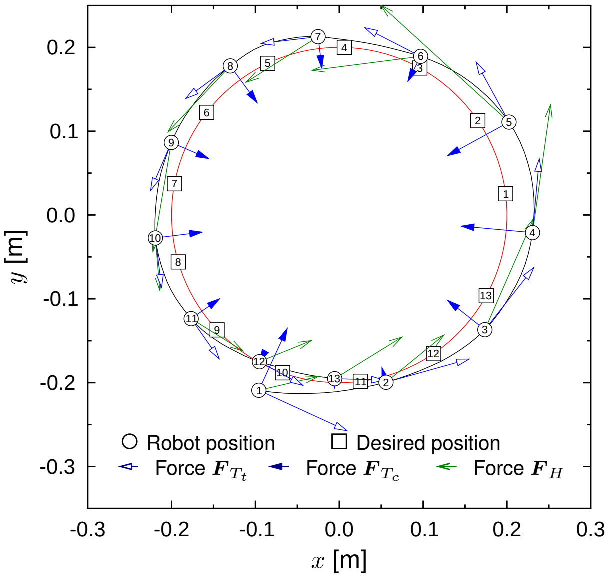

Figure 6: Tracking test: force vectors and positions.

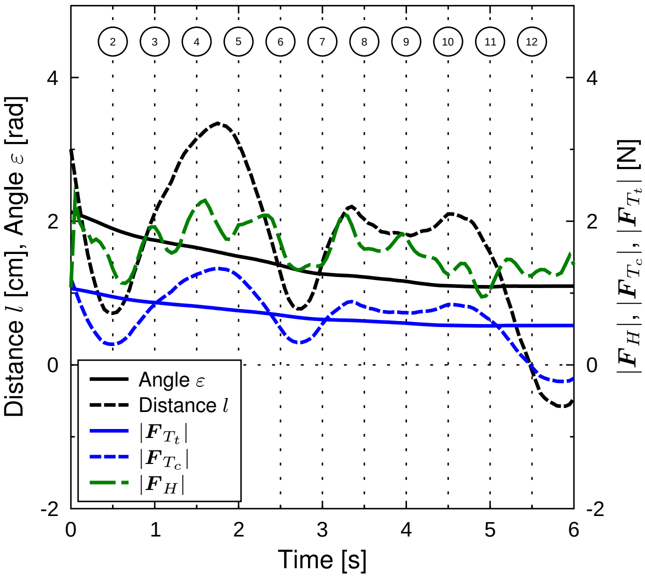

Figure 7: Tracking test: force magnitudes, l, ε.

6 Experimental Results

The haptic controller including the virtual therapist has been successfully tested in experiments with neurologically intact subjects. The Figures 6 and 7 show data from a test in which a moving point on a circle (radius of 0.2 m, frequency of 0.15 Hz) had to be tracked by the test person. Using haptic control, a virtual mass of 0.5 kg and a virtual damping of 10 Ns/m have been realised for the robot. The spring constants of the virtual therapist were set to $k_l = 40$ N/m and $k_\varepsilon = 0.5$ N/rad. It can be clearly seen from Figure 6 that the virtual therapist supports the movement tangentially to the circle. On the contrary, radial deviations from the circle are kept small by the virtual therapist.

7 Conclusion

The feasibility to realise haptic control for a table-placed mobile rehabilitation robot was initially demonstrated in experiments with healthy subjects. Further work includes the design of a proper arm support, the integration of power supply and electronics onto the *Reha-Maus* and the replacement of the infrared camera by a robot-mounted absolute position sensor before carrying out clinical tests with patients. The entire safety concept of the system as well as the possible problem of wheel slipping in presence of large disturbances are currently under investigation. The latter may be an issue in patients with significant spasticity.

References

[1] H. I. Krebs, N. Hogan, M. L. Aisen and B. T. Volpe, “Robot-aided neurorehabilitation”, IEEE Transactions on Rehabilitation Engineering, Vol. 6, No. 1, pp. 75–87, March, 1998.

[2] Nef T. and R. Riener, “ARMin – design of a novel arm rehabilitation robot”, IEEE International Conference on Rehabilitation Robotics, Chicago, 2005, pp. 57-60.

[3] X. Chen and M. King, “Automated variable resistance system for upper limb rehabilitation”, Australasian Conference on Robotics and Automation (ACRA), December 2-4, 2009, Sydney, Australia.

[4] J. C. Perry, H. Zabaleta, A. Belloso and T. Keller, “ARMassist: a low-cost device for telerehabiltation of post-stroke arm deficits ”, World Congress on Medical Physics and Biomedical Engineering, September 7- Sep 12, 2009, Munich, Germany.

[5] D. Luo, M. Roth, C. Wiesener, T. Schauer, H. Schmidt and J. Raisch, “*Reha-Maus*: A Novel Robot for Upper Limb Rehabilitation”, Workshop Automed 2010, October 29-30, 2010, Zuerich, Switzerland.

Acknowledgments: The authors thank Henning Schmidt from the Fraunhofer IPK Berlin, German, Automation Technology Division, Rehabilitation Robotics Group, for his advice during the development of the *Reha-Maus* and further co-operation.

Contact: Thomas Schauer, E-Mail: schauer@control.tu-berlin.de